J|A|C|S
ARTICLES
Published on Web 09/10/2004

Excited-State Proton Transfer Reactions of 10-Hydroxycamptothecin[1]

Kyril M. Solntsev,*,† Erica N. Sullivan,†,‡ Laren M. Tolbert,*,† Shay Ashkenazi,§ Pavel Leiderman,§ and Dan Huppert§

Contribution from the School of Chemistry and Biochemistry, Georgia Institute of Technology, Atlanta, Georgia, 30332-0400, and Raymond and Beverly Sackler Faculty of Exact Sciences, School of Chemistry, Tel Aviv University, Tel Aviv 69978, Israel

Received April 15, 2004; E-mail: solntsev@chemistry.gatech.edu; tolbert@chemistry.gatech.edu

Abstract: Time-resolved and steady-state emission characterization of 10-hydroxycamptothecin reveals a rich but less complex proton-transfer behavior than its parent hydroxyquinoline. The electronic effect of the additional electron-withdrawing ring makes the excited-state both less basic and more acidic than the parent and adds to the class of high-acidity excited-state proton donors in photochemistry and photobiology.

1. Introduction

Camptothecin (**CPT**) is a pentacyclic alkaloid first isolated from extracts of the Chinese tree *Camptotheca acuminata*. This brightly fluorescent compound was found to be a potent inhibitor of the growth of leukemia cell by a unique mechanism: inhibition of DNA topoisomerase I.[2a,b] A Mannich derivative, topotecan (**TPT**), is now used in the treatment of ovarian cancer. The natural fluorescent properties of **CPT** and its derivatives have been exploited to monitor its concentration in living cells.[2] Significant attention has been paid to the equilibrium between the lactone and its ring-opened carboxylate form, which influences its antitumor ability.

Among the wide variety of **CPT** derivatives, two moderately water-soluble compounds, 10-hydroxycamptothecin (**10-CPT**) and 7-ethyl-10-hydroxycamptothecin (**SN-38**), as well as **TPT**, contain the 6-hydroxyquinoline (**6HQ**) subunit (see Figure 1). Hydroxyquinoline derivatives are known to be both strong photoacids and strong photobases, and therefore, they undergo efficient tautomerization in a wide pH range resulting in weak tautomer (zwitterion) emission.[3,4] Because of our interest in the acid−base properties of photoexcited molecules[5] and, in particular, because of the relative paucity of such examples in the biological literature, we were particularly interested in reports

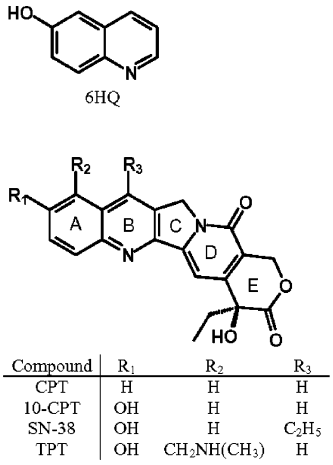

Compound	R_1	R_2	R_3
CPT	H	H	H
10-CPT	OH	H	H
SN-38	OH	H	C_2H_5
TPT	OH	$CH_2NH(CH_3)$	H

Figure 1. **CPT** and its hydroxyderivatives with the conventional ring numbering system.

of anomalous behavior that might involve excited-state prototropic processes. Proton transfer, both in ground and excited states, plays a key role in many biological processes. It is not surprising that the functioning of many biological objects depends on the pH of the media within and outside them. The problem of determination of static pH in this medium as well as proton translocation is being successfully solved using various artificial pH probes.[6] On the other hand, less is known about excited-state proton transfer (ESPT) observed in naturally occurring systems. It is interesting to note that the overall action of light on several such systems is completely different, though ESPT is an important step in all of them: Upon irradiation, several photoproteins such as Green Fluorescent Protein[7] or obelin[8] demonstrate bioluminescence; a transmembrane protein bacteriorhodopsin acts as a light-driven proton pump in convert-

† Georgia Institute of Technology.

‡ Current address: Materials and Processes Branch, NASA−Johnson Space Center, Houston, TX 77058.

§ Tel Aviv University.

(1) This is part of our series "Photochemistry of 'super' photoacids". For a previous article, see: Clower, C.; Solntsev, K. M.; Kowalik, J.; Tolbert, L. M.; Huppert, D. *J. Phys. Chem. A* **2002**, *106*, 3114−3122.

(2) (a) *Camptothecins: New Anticancer Agents*; Potmesil, M., Pinedo, H., Eds.; CRC Press: Boca Raton, FL, 1995. (b) Garcia-Carbonero, R.; Supko, J. G. *Clin. Cancer Res.* **2002**, *8*, 641−661. (c) Croce, A. C.; Bottiroli, G.; Supino, R.; Favini, E.; Zuco, V.; Zunino, F. *Biochem. Pharm.* **2004**, *67*, 1035−1045.

(3) Bardez, E.; Châtelain, A.; Larrey, B.; Valeur, B. *J. Phys. Chem.* **1994**, *98*, 2357−2366.

(4) (a) Kim, T. G.; Kim, Y.; Jang, D.-J. *J. Phys. Chem. A* **2001**, *105*, 4328−4332. (b) Poizat, O.; Bardez, E.; Buntinx, G.; Alain, V. *J. Phys. Chem. A* **2004**, *108*, 1873−1880.

(5) Tolbert, L. M.; Solntsev, K. M. *Acc. Chem. Res.* **2002**, *35*, 19−27.

(6) *Handbook of Fluorescent Probes and Research Products*, 9th ed.; Haughland, R. P., Ed.; Molecular Probes: Eugene, OR, 2002; Ch. 21.

(7) Zimmer, M. *Chem. Rev.* **2002**, *102*, 759−781.

(8) Malikova, N. P.; Stepanyuk, G. A.; Frank, L. A.; Markova, S. V.; Vysotski, E. S.; Lee, J. *FEBS Lett.* **2003**, *554*, 184−188.

ing light energy to a proton gradient;[9] and several chloroplasts demonstrate phototropism, a light-directed movement and light-induced stomatal opening, all controlled by plant photoreceptor kinases.[10] In some cases, proton transfer is coupled to electron transfer, as in the case of photosynthesis[11] and DNA photooxidation.[12] ESPT was also detected in simpler chromophores isolated from biological systems or their synthetic analogues.[13] We now report evidence on the occurrence of such behavior in a hydroxy derivative of **10-CPT** and, additionally, provide information on the dynamics of this process.[14]

The camptothecin choromophore consists of five fused rings (Figure 1). The A/B rings contain the quinoline ring system, while the pyridone ring D exerts significant electron-withdrawing effects. In the past decade a lot of effort has been made to establish the electronic and vibronic structure of **CPT** chromophores using UV−vis absorbance and fluorescence spectroscopy, as well as Raman spectroscopy.[15−19] We note the following important features of **CPT** derivatives that are relevant for the investigation of **10-CPT** photochemistry at our experimental conditions:

(1) In aqueous solutions the ring E lactone hydrolyses, forming the carboxylate. The pK_a of the carboxylic group in **CPT** is about 6.5. The rate of hydrolysis and the lactone−carboxylate equilibrium constant strongly depend on pH, temperature, and microenvironment, but generally the half-life of the lactone form of various **CPT** derivatives in homogeneous buffer solutions at neutral pH is tens of minutes. For various **CPT** derivatives, the hydrolysis causes a weak (ca. 5 nm) bathochromic shift in the absorption spectra. The concurrent fluorescence change is also weak. The emission peak has a small bathochromic shift (up to 15 nm), and the fluorescent quantum yield decreases by less than 10%.

(2) **CPT** derivatives can be protonated at the quinoline nitrogen. The protonation results in the appearance of quinolinium-type red-shifted absorption ($\Delta\lambda = 35-40$ nm)[16a,17b] and emission ($\Delta\lambda = 80$ nm)[16a] bands. The pK_a of the ground-state protonation was about 0.7 for **CPT** and 1.8 for **SN-38**. In contrast to quinoline derivatives,[20] the **CPT** does not behave like a strong photobase and the pK_a* for quinolinium nitrogen deprotonation is only 1.64.[16a]

(3) **CPT** and some of its derivatives demonstrate single-peak fluorescence in organic as well as in neutral and basic aqueous solvents. In contrast, the addition of a hydroxyl substituent at the 10-position (A-ring) causes a decrease in fluorescence quantum yield and the appearance of a dominant red-shifted ($\Delta\lambda = 150$ nm) emission. Mi and Burke considered **10-CPT** dual fluorescence in methanol−water mixtures as solvent polarity-dependent without taking into account any possible excited-state proton transfer.[18b] Chourpa et al.[17c] were more specific, attributing the dual **SN-38** fluorescence as a result of the increased phenol-type acidity.

2. Experimental Section

6-Hydroxyquinoline was purchased from Aldrich. 10-Hydroxycamptothecin having 99% purity was purchased from ICN Pharmaceutical. Spectroscopic measurements were carried out in methanol−water mixtures prepared by the volumetric method. The methanol solvent was BDH HPLC grade with <0.05% water. Deionized water (resistivity >10 MΩ/cm) was used for dilutions. Solvents contained no detectable fluorescent impurities and were used without further purification. All experiments were performed at room temperature (ca. 22 °C). Steady-state fluorescence spectra of nondeoxygenated **10-CPT** solutions were recorded on a SPEX spectrofluorometer. CD spectra were determined using a JASCO J-810 CD spectropolarimeter. Transient fluorescence was detected using time-correlated single-photon counting. A synchronized, cavity-dumped picosecond Rhodamine 6G dye laser, driven by a Nd:YAG laser, was used as a source of excitation. The time resolution varied from 4.88 to 97.7 ps/channel, while the instrument response function (IRF) at the short time scales had a full-width at half-maximum (fwhm) of about 40 ps. For the pump−probe experiments we used an amplified Ti:Sapphire laser system. Laser pulses (50 fs duration, centered near 800 nm with a pulse energy of ~600 μJ) with a 1 kHz repetition rate were generated by a Ti:Sapphire-based oscillator and amplified by a multipass Ti:Sapphire amplifier. Samples were excited by the second harmonic of the amplified laser (~390 nm). The cross correlation between the pump and the probe pulses was measured to be 250 fs fwhm. Time-resolved data from the solutions were obtained using a femtosecond pump−probe technique with a time resolution of about ~150 fs, as well as time-correlated single photon counting (TCSPC) with a limited time resolution of about 20 ps after deconvolution.[21] Semiempirical calculations were performed with the Spartan Pro implementation of the AM1 method.[22]

3. Results

3.1. Spectroscopic Measurements and pH Titrations. Although **10-CPT** is moderately soluble in neutral water in its lactone form, it tends to aggregate.[17a] Thus, the study of the pH dependence of emission and absorbance in methanol−water mixtures is required to avoid aggregation. Absorption and emission spectra of **6HQ** in water at various pH and its mixtures with methanol are presented in the literature,[3,4] but no spectral data exists for the pH dependence of **6HQ** spectra in 1/1 vol methanol−water. In this solvent the dissociation constants for

(9) Lanyi, J. K. *Annu. Rev. Physiol.* **2004**, *66*, 665−688.
(10) Kennis, J. T. M.; Crosson, S.; Gauden, M.; van Stokkum, I. H. M.; Moffat, K.; van Grondelle, R. *Biochemistry* **2003**, *42*, 3385−3392.
(11) Paddock, M. L.; Feher, G.; Okamura, M. Y. *FEBS Lett.* **2003**, *555*, 45−50.
(12) Shafirovich, V.; Geacintov, N. E. *Top. Curr. Chem.* **2004**, *237*, 129−157.
(13) (a) Guharay, J.; Sengupta, P. K. *Spectrochim. Acta, Part A* **1997**, *53*, 905−912. (b) Das, K.; Ashby, K. D.; Wen, J.; Petrich, J. W. *J. Phys. Chem. B* **1999**, *103*, 1581−1585. (c) Reyman, D.; Viñas, M. H.; Camacho, J. J. *J. Photochem. Photobiol., A* **1999**, *120*, 85−91. (d) Il′ichev, Y. V.; Perry, J. L.; Manderville, R. A.; Chignell, C. F.; Simon, J. D. *J. Phys. Chem. B* **2001**, *105*, 11369−11376. (e) Altucci, C.; Borrelli, R.; de Lisio, C.; de Riccardis, F.; Persico, V.; Porzio. A.; Peluso, A. *Chem. Phys. Lett.* **2002**, *354*, 160−164.
(14) A preliminary report of this work has appeared: Ashkenazi, S.; Leiderman, P.; Huppert, D.; Solntsev, K. M.; Tolbert, L. M. In *Femtochemistry and Photobiology*; Martin, M. M., Hynes, J. T., Eds., Elsevier: Amsterdam, 2004, pp 201−206.
(15) Fassberg, J.; Stella, V. J. *J. Pharm. Sci.* **1992**, *81*, 676−684.
(16) (a) Dey, J.; Warner, I. M. *J. Photochem. Photobiol., A* **1996**, *101*, 21−27. (b) Dey, J.; Warner, I. M. *J. Lumin.* **1997**, *71*, 105−114. (c) Dey, J.; Warner, I. M. *J. Photochem. Photobiol., A* **1998**, *116*, 27−37. (d) Biswas, A.; Dey, J. *Indian J. Chem., Sect. A* **2001**, *40A*, 1143−1148.
(17) (a) Fleury, F.; Kudelina, I.; Nabiev, I. *FEBS Lett.* **1997**, *406*, 151−156. (b) Nabiev, I.; Fleury, F.; Kudelina, I.; Pommier, Y.; Charton, F.; Riou, J.-F.; Alix, A. J. P.; Manfait, M. *Biochem. Pharmacol.* **1998**, *55*, 1163−1174. (c) Chourpa, I.; Millot, J.-M.; Sockalingum, G. D.; Riou, J.-F.; Manfait, M. *Biochim. Biophys. Acta* **1998**, *1379*, 353−366. (d) Chourpa, I.; Riou, J.-F.; Millot, J.-M.; Pommier, Y.; Manfait, M. *Biochemistry* **1998**, *37*, 7284−7291. (e) Chauvier, D.; Chourpa, I.; Maizieres, M.; Riou, J.-F.; Dauchez, M.; Alix, A. J. P.; Manfait, M. *J. Mol. Struct.* **2003**, *651*, 55−65.
(18) (a) Burke, T. G.; Mi, Z. *J. Med. Chem.* **1994**, *37*, 40−46. (b) Mi, Z.; Burke, T. G. *Biochemistry* **1994**, *33*, 10325−10336. (c) Mi, Z.; Burke, T. G. *Biochemistry* **1994**, *33*, 12540−12545. (d) Burke, T. G.; Malak, H.; Gryczynski, I.; Mi, Z.; Lakowicz, J. R. *Anal. Biochem.* **1996**, *242*, 266−270.
(19) Posokhov, Y.; Biner, H.; Içli, S. *J. Photochem. Photobiol., A* **2003**, *158*, 13−20.
(20) Weller, A. *Prog. React. Kinet.* **1961**, *1*, 189−214.
(21) Genosar, L.; Cohen, B.; Huppert, D. *J. Phys. Chem. A* **2000**, *104*, 6689−6698.
(22) Available from Wavefunction, Inc.

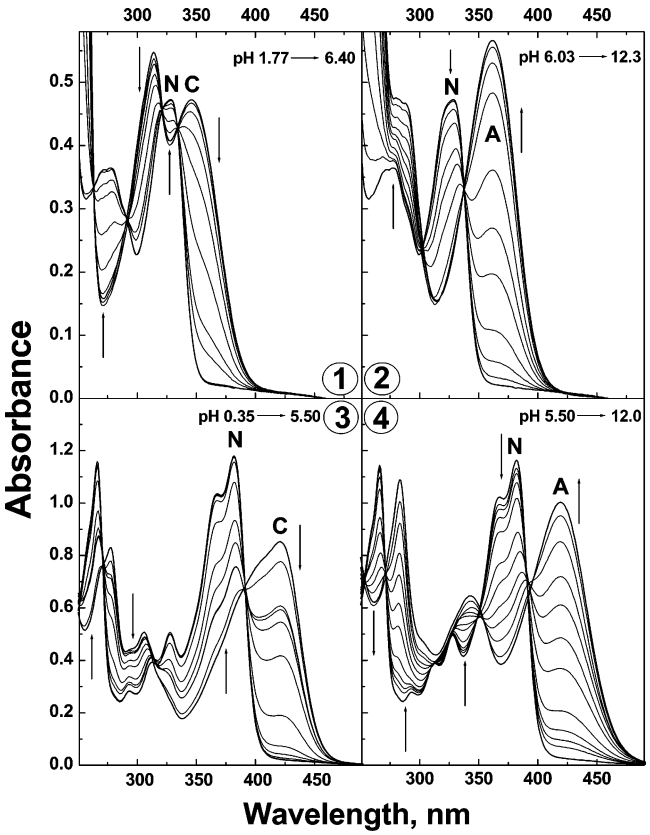

Figure 2. Absorption spectra of **10-CPT** and **6HQ** in 1/1 v/v water−methanol mixture as function of pH. (1) **6HQ** in acidic pH region. (2) **6HQ** in basic pH region. (3) **10-CPT** in acidic pH region. (4) **10-CPT** in basic pH region. Absorbance bands of neutral, cationic, and anionic species are marked as N, C, and A, respectively.

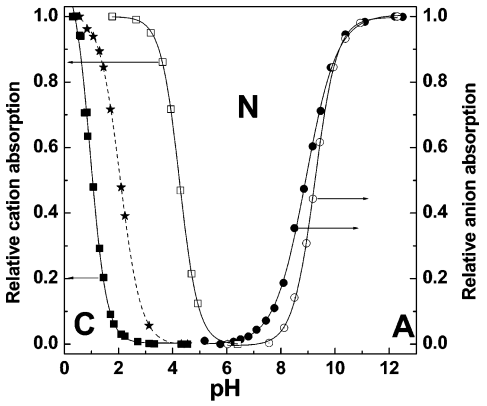

Figure 3. Steady-state titrations curves of **6HQ** and **10-CPT** in 1/1 v/v water−methanol mixture. (□ and ○) Absorbance data for **6HQ**. (■ and ●) Absorbance data for **10-CPT**. (★) Inverse relative anionic emission of **10-CPT** at 520 nm. N, C, and A are the integrated absorptions of the neutral, cationic, and anionic species, respectively.

many phenols increase by 0.3−1.0 pK_a unit as compared to bulk water, while dissociation constants of protonated amines decrease, but less significantly.[23]

Solution pH measurements were performed in 1/1 v/v methanol−water mixtures (0.692 molar fraction H_2O) with a glass electrode precalibrated in aqueous buffer.[24] The absorption spectra of **10-CPT** in 1/1 v/v water−methanol at neutral pH were close to that of **SN-38**.[17] With a pH increase from 5.5 to 12.0, the peak with the maximum at 381 nm disappeared and a new peak with a maximum at 419 nm arose (Figure 2). The absorption spectra in neutral water and methanol were nearly identical, the latter having a 3-nm bathochromic shift. Similar behavior was observed for **6HQ** (Figure 2). In acidic media another type of transition was observed. With a pH decrease from 5.5 to 0.35, the peak at 381 nm was transformed into a new peak with a maximum at 421 nm (Figure 2).

The two absorptions were well-separated enough for independent determinations of the dissociation constant in each case. For the sake of the discussion later, we will associate the low pH dissociation constant with protonation at nitrogen and the high pH constant with deprotonation at oxygen. Also for the sake of comparison with **10-CPT**, we determined acid−base constants of the parent 6-hydroxyquinoline in the 1/1 v/v MeOH−water mixture as well. We assumed that ΔpK_a values between water and 1/1 v/v MeOH−water mixtures were similar for **6HQ** and **10-CPT**.

The titration curves are presented in Figure 3. The acidity constant (pK_a) values calculated from the titration data are as follows:

	$-NH^+ \leftrightarrow -N + H^+$	$-OH \leftrightarrow -O^- + H^+$
6HQ	4.25	9.25
10-CPT	0.96	8.96

There is no literature data on the kinetics and thermodynamics of lactone hydrolysis of **10-CPT** in methanol−water mixtures, and therefore it was important to establish the possibility of this process in our system. As was mentioned earlier, lactone and carboxylate forms of **CPT** hydroxyderivatives are practically nondistinguishable in UV-absorbance and fluorescence spectra.[17c] Thus, similar to the method described in ref 17, we used CD spectroscopy to detect optically active spectra of **10-CPT** lactone and carboxylate, which are known to differ in the sign of CD bands in the region of 325−400 nm. A modest signal-to-noise ratio in the CD spectra did not allow us to make precise quantitative estimates. However, similar to results of ref 17, we observed a decrease with time in the amplitude of a negative signal at 350 nm of freshly prepared methanol−water solutions of **10-CPT** due to lactone hydrolysis, leading to CD signal inversion. For example, in 0.56 mol fraction H_2O/MeOH solution the signal at 350 nm changed from −2 to −0.7 $\Delta\epsilon_M$ M^{-1} cm^{-1} in 40 min after solution preparation. From the known data on **CPT** CD spectra,[17b] we estimate that ca. 20−30% of **10-CPT** lactone was hydrolyzed.

3.2. Emission Spectra and Time-Resolved Measurements. In contrast to the similar ground-state properties of **6HQ** and **10-CPT**, the emission properties of **10-CPT** differed strongly from that of **6HQ**. For instance, unlike **6HQ**,[25] the spectra of **10-CPT** exhibited dual fluorescence (Figure 4) even in bulk methanol, while **6HQ** showed no ESPT. With the addition of water, we observed a substantial decrease in the fluorescence intensity of the high-energy band at 430 nm and a concomitant increase of the band at 570 nm. A clear isoemissive point at

(23) Rosés, M.; Rived, F.; Bosch, E. *J. Chromatogr., A* **2000**, *867*, 45−56.
(24) (a) Bosch, E.; Bou, P.; Allemann, H.; Rosés, M. *Anal. Chem.* **1996**, *68*, 3651−3657. (b) Avdeef, A.; Box, K. J.; Comer, J. E. A.; Gilges, M.; Hadley, M.; Hibbert, C.; Patterson, W.; Tam, K. Y. *J. Pharm. Biomed. Anal.* **1999**, *20*, 631−641. (c) Canals, I.; Portal, J. A.; Bosch, E.; Rosés, M. *Anal. Chem.* **2000**, *72*, 1802−1809. (d) Canals, I.; Valko, K.; Bosch, E.; Hill, A. P.; Rosés, M. *Anal. Chem.* **2001**, *73*, 4937−4945. (e) Canals, I.; Oumada, F. Z.; Rosés, M.; Bosch, E. *J. Chromatogr., A* **2001**, *911*, 191−202.
(25) Mehata, M. S.; Joshi, H. C.; Tripath, H. B. *Chem. Phys. Lett.* **2002**, *359*, 314−320.

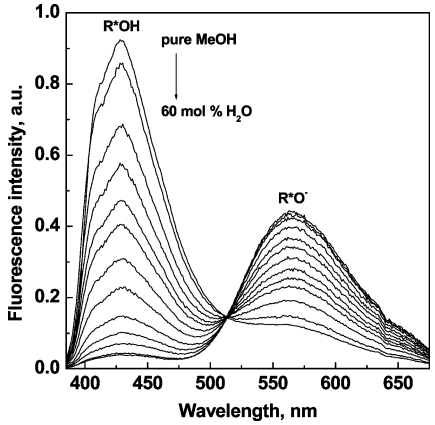

Figure 4. Emission spectra of **10-CPT** in methanol−water mixtures. Water molar fractions (from top to bottom for R*OH band at 430 nm) are: 0, 00067, 0.035, 0.05, 0.063, 0.075, 0.098, 0.132, 0.189, 0.269, 0.37, 0.539, and 0.6. $\lambda_{ex} = 384$ nm.

Table 1. Parameters Used in Fitting the Time-Resolved Fluorescence Decay of 10-CPT Measured Using TCSPC and Pump−Probe Techniques, and Calculated pK_a* Values in MeOH/H_2O Mixtures[a]

$X(H_2O)$[b]	k_d (ns^{-1})	k_a (Å ns^{-1})	k_{rl} (Å ns^{-1})	R_D (Å)[c]	R_D^{eff} (Å)[d]	D (10^{-5} cm^2 s^{-1})[c]	pK_a*[e]
			TCSPC				
0	0.48	5.0	2	17.2	17.2	3.50	1.74
0.069	1.45	4.5	6	16.4	22	2.20	1.15
0.124	2.7	5.0	10	15.8	19	2.05	0.87
0.175	4.0	5.5	11	15.2	18	2.00	0.70
0.297	7.5	6.0	11	13.7	17.5	2.10	0.34
0.458	18	8.0	11	11.9	16.5	2.60	−0.05
0.560	28	11	13	10.8	16	3.00	−0.19
0.717	40	15	15	9.4	15	4.20	−0.33
			Pump−Probe				
0	0.5	4.5	2	17.2	17.2	3.5	1.74
0.18	4.2	5.7	10	13.6	15.0	2.0	0.68
0.4	17	7.6	11	11.0	12.8	2.36	0.07
0.67	37	13	13	8.8	10.2	3.80	−0.28
0.75	65	16	16	8.3	8.7	4.6	−0.56
0.87	85	20	20	7.7	8.0	6.7	−0.64

[a] Lifetime of R*OH was assumed to be 6.7 ns (lifetime in polar nonbasic solvents) and lifetime of R*O$^-$ was determined to be constant of 5.05 ns at all water concentrations and in basic methanol solution. [b] Mole fraction of water. [c] Debye radii and diffusion coefficients were estimated as described in ref 28. [d] Effective Debye radii that take into account lactone hydrolysis. See text for details. [e] Calculated as $pK_a^* = -\log[k_d 10^{27} \exp(-R_D/a)/(k_r N_A)]$, the value of the contact radius in the ion pair a was assumed to be 5.5 Å.[28]

519 nm was detected at water content from 0 up to 0.6 mole fraction. At higher water concentrations the fluorescence spectra had the same band ratio as in the latter solution, but their intensity decreased.

The time-resolved signals from R*OH and R*O$^-$ at various water concentrations were detected at 420 and 590 nm, corresponding to a minimal overlap between R*OH and R*O$^-$ emission bands (see Figure 4). Experimental curves were fitted to the numerical solutions of the time-dependent Debye−Smoluchowski equation (DSE) using the SSDP program used previously.[26] The fitting parameters are presented in Table 1. Figure 5 shows an example of the experimental kinetic data fitting. Here, the dots are the time-resolved emission data for **10-CPT** in 0.124 molar fraction of H_2O−MeOH mixture, and the solid curves are the theoretical calculations for both acidic and anionic forms of **10-CPT** convoluted with the IRF. Both

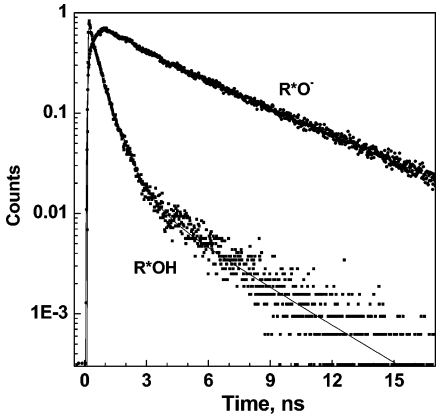

Figure 5. Time-resolved kinetics of **10-CPT** in 0.124 molar fraction H_2O−MeOH mixture. Experimental data points (normalized to the theoretical amplitudes) are compared with the numerical solution of the DSE (lines) using the parameters of Table 2, after convolution with IRF.

R*OH and R*O$^-$ kinetics were fitted simultaneously using the same kinetic parameters listed in Table 1.

Because of the limited time resolution of the TCSPC technique, we also studied ultrafast ESPT in water-rich mixtures using a femtosecond pump−probe technique. We have demonstrated earlier[27] that pump−probe signals from photoacids may have a complex nature due to heavy mixing of $S_1 \rightarrow S_n$ absorption of R*OH, R*O$^-$ and stable photoproducts on one hand and stimulated emission from these species on the other hand. Careful choice of excitation laser power and detection wavelength may minimize unnecessary overlaps. Transient absorption signals of **10-CPT** in 1/1 vol MeOH−water were measured at various wavelengths from 480 to 600 nm. From 480 nm up to about 540 nm, the signal was positive from time 0 to 80 ps; at longer times only a slight decay was observed. From 550 to 600 nm, the signal was positive at short times and negative at longer times. In this wavelength range only two dominating processes were observed. The first one that led to an increase in the pump−probe signal was the ultrafast absorption occurring instantaneously and not carrying any important kinetic information. The second one was the stimulated emission of R*O$^-$ leading to a decrease of the overall pump−probe signal. We chose detection at 590 nm to minimize overlap between the stimulated emission of R*O$^-$ and other satellite processes; note that this was also the wavelength for monitoring R*O$^-$ emission using TCSPC technique. As a result, we found good correspondence between the long time component of the pump probe signal and the TCSPC signal. Figure 6 shows the pump−probe signal of **10-CPT** in water−methanol mixtures measured at 590 nm after excitation of the sample by a ∼100 fs pulse at 390 nm. As seen, the larger the water mole fraction, the faster the decay rate. At the highest water mole fraction, the probe pulse transmission, ΔT, changes signs from $\Delta T < 0$ to $\Delta T > 0$ at about 20 ps. The signal consists of two distinct time regimes, a short-time component of amplitude of about 0.2 and 3 ps lifetime, and a long-time component of about 14 ps at $x_{H2O} \approx 0.8$.

With decreasing pH, the simultaneous quenching of both fluorescence bands was observed, and the two-band spectra transformed into single-band emission with a maximum around

(26) Krissinel, E. B.; Agmon, N. *J. Comput. Chem.* **1996**, *17*, 1085−1098.

(27) Cohen, B.; Leiderman, P.; Huppert, D. *J. Lumin.* **2003**, *102−103*, 682−687.

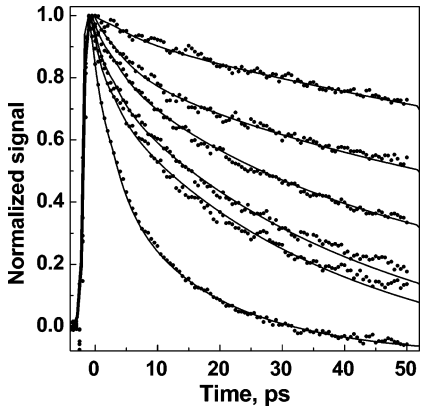

Figure 6. Pump−probe signal of **10-CPT** in methanol−water mixtures. The pump was at 390 nm, and the probe was at 590 nm. Water mole fraction top to bottom: 0, 0.18, 0.28, 0.40, 0.48, and 0.84.

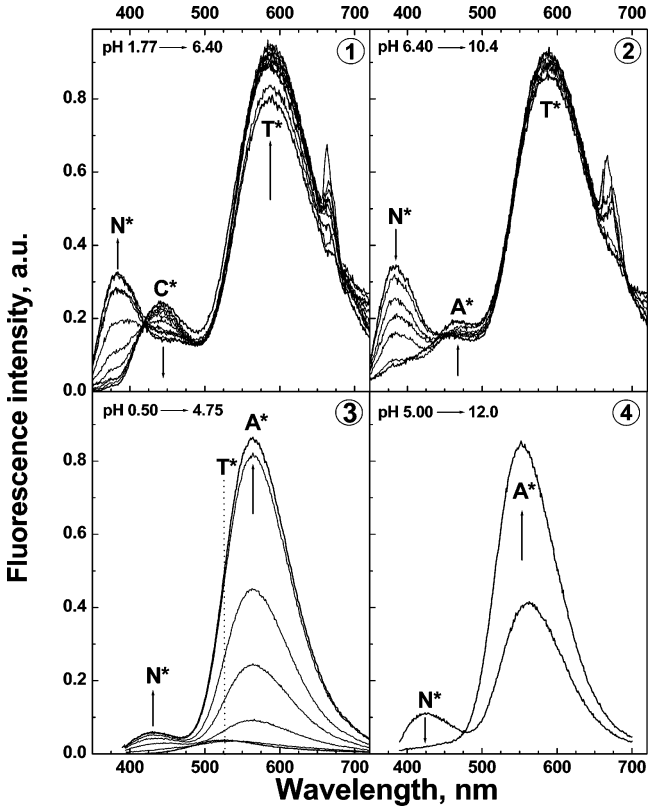

Figure 7. Emission spectra of **10-CPT** and **6HQ** in 1/1 v/v water−methanol mixture as function of pH. (1) **6HQ** in acidic pH region. (2) **6HQ** in basic pH region. (3) **10-CPT** in acidic pH region. (4) **10-CPT** in basic pH region. In all cases, the excitation wavelengths were long-wavelength isosbestic points for corresponding acid−base transitions. Emission bands of the excited neutral, cationic, anionic, and tautomer species are marked as N*, C*, A*, and T*, respectively.

525 nm (Figure 7). The inflection point at the titration curve was observed around pH 2.0 (Figure 3). Upon further acidification up to 5.5 M $HClO_4$, no dramatic changes in emission were observed; the emission maximum did not change, and the intensity increased by 30%. This differs significantly from the pH dependence of **6HQ** emission spectra. In the latter case, a pH decrease from 6.0 to 1.77 did not influence the dominating tautomer peak, and the emission of neutral form transferred into the cationic form due to ground-state protonation[3] (Figure 7). In very acidic solutions, the emission peak increased significantly.

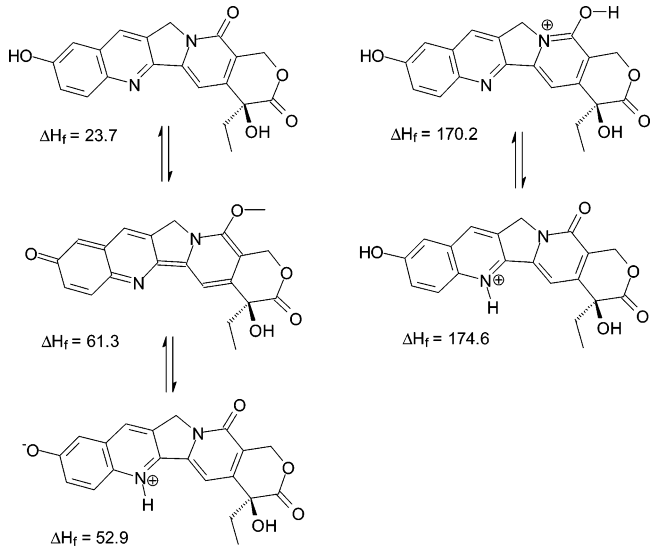

Figure 8. Gas-phase heats of formation predicted for various **10-CPT** tautomers and their conjugate acids by AM1.

With increasing pH, the emission band of **10-CPT** at 430 nm totally converted into a long-wavelength emission at 575 nm. Upon addition of NaOH up to pH 12, the emission maxima of the latter exhibited a minor 5-nm hypsochromic shift. Under the same conditions, the dominating emission of **6HQ** was from the tautomer. The emission of the neutral form transferred into the anionic form because of ground-state deprotonation[3] (Figure 7).

4. Discussion

4.1 Steady-State Spectra. At neutral pH, we associate the 381-nm absorption of **10-CPT** with the neutral species, and at high pH, we associate the 419-nm absorption with the deprotonated species. It is important to realize that two acid−base processes occur in this pH region: E-ring lactone hydrolysis and deprotonation of A-ring hydroxyl. Both lead to the appearance of low-energy absorbance bands. However, as was mentioned in the Introduction, the magnitude of the shift in the first case is almost negligible, and therefore, the observed effect is due to A-ring hydroxyl deprotonation. Overlap of two transitions is probably the reason for the diffuse isosbestic point (Figure 2). The equilibrium between neutral (ROH) and O-deprotonated (RO^-) forms of **10-CPT**, characterized by a pK_a of 8.9 (Figure 3), is close to that of **SN-38**[17a] and parent **6HQ** in water.[3]

At low pH, for the 421-nm absorption, several alternatives can be considered due to the presence of several acid−base centers in **10-CPT**. It is generally accepted[15−17] that the appearance of this peak in **CPT** derivatives is due to protonation of the B-ring quinoline nitrogen. This equilibrium process has a pK_a around 1.0, more than 3 pK_a units lower than in the parent **6HQ** (Figure 3) and similar to all **CPT** derivatives studied.[15−17] The much lower ground-state basicity of the quinoline nitrogen in **CPT** and its derivatives can be explained by the electron-withdrawing effect of the conjugated pyridone ring.[15,16a] For this reason, one might also consider protonation on the carbonyl oxygen of the pyridone ring (see Figure 8). Indeed, semiempirical (AM1) calculations indicate that protonation at oxygen is favored by ca. 4.4 kcal/mol. However, given the significant differences in the solvation energies we would expect for the

two tautomers, we cannot provide irrefutable information on the structure of the protonated species.

From these data one can see that the reason for poor ground and excited basicity of **10-CPT** is the electronic structure of molecule, namely, the electron-withdrawing nature of the D ring. Thus, the ground-state behavior of **10-CPT** (and **SN-38**[17b]) resembles that of **6-HQ**, with modifications due to the relative pK_a's. Depending on pH, three *major* ground-state species can exist: an N-protonated quinolinium cation (alternatively, hydroxypyridinium), neutral molecule, and O-deprotonated phenolate (Figure 3). In addition, the E-ring in **CPT**s may exist in lactone and carboxyl forms at solutions at pH close to neutral, and we attribute the ca. 5-nm hypsochromic shift to lactone ring opening. However, this transition is almost invisible against the background of hydroxyl deprotonation.

Similar spectral behavior for this system was demonstrated by Mi and Burke,[18b] who proposed that microenvironment polarity is the main determinant of the emission spectral properties. No assumptions about the nature of the emission bands and mechanism of the excited-state processes were given. Chourpa et al. were more specific in giving the reasons for dual fluorescence on **SN-38** in DMSO−water mixtures,[17c] proposing that the low-energy emission is from the phenolate formed as a result of the excited-state proton transfer to solvent.

The appearance of the low-energy emission band at 570 nm for **10-CPT** in neat methanol solution indicates an efficient ESPT process and a significant excited-state acidity. The large fluorescence quantum yield in methanol−water mixtures and similarity of the emission maxima at neutral and basic (pH 12) solutions is evidence of the excited anion (R^*O^-) formation, in contrast to **6HQ**, for which a double excited-state proton transfer leads to a tautomer as the dominant species.[3,4] In the latter case, upon further addition of NaOH up to 5 M concentration, the emission of **6HQ** shifted to shorter wavelength, i.e., from a tautomer to purely anionic emission[3] (data not shown, see Figure 7 in ref 3), while the emission maxima and intensity of **10-CPT** remained the same. Therefore, we conclude that the excited-state prototropic behavior of **10-CPT** in neutral and basic solutions is much simpler than for **6HQ** and does not involve an aromatic quinolinium nitrogen as a strong photobase in the excited state. This means that ESPT involves only deprotonation of the A-ring hydroxyl group. Therefore, the spectral behavior of **10-CPT** in methanol−water mixtures as shown in Figure 4 can be attributed to the well-known increase of the protolytic photodissociation rate with increasing water concentration.[28] In contrast to the ground-state properties, the excited-state properties of **6HQ** differ strongly from that of **10-CPT**. The former compound shows no ESPT in dry methanol, but in water in very wide pH range from 0 to 12 it demonstrates very weak fluorescence from tautomer (zwitterion) formed as the result of double proton transfer coupled to intramolecular charge transfer (Figure 7).[3,4]

4.2. Time-Resolved Emission Data. On the basis of these conclusions, we may apply our kinetic scheme for protolytic photodissociation of hydroxyaromatic compounds (Scheme 1) for the analysis of **10-CPT** excited-state behavior. For simplicity, we will consider R*OH as an averaged population of the excited **10-CPT** in both lactone and carboxylate forms, but with

Scheme 1

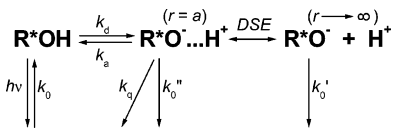

protonated phenolic proton of ring A. As was mentioned earlier, lactone and carboxylate forms of **CPT** hydroxyderivatives are practically nondistinguishable in UV spectra,[17c] and their lifetimes measured in R^*O^- band are the same.[18] We assume that both the lactone and the carboxylate forms of **10-CPT** have very close spectral, kinetic, and diffusion parameters except for the charge. In this case, the apparent fluorescence signal assumes an "effective" charge of this molecule, reflecting the ground-state equilibrium caused by slow hydrolysis.

Because of the complex behavior of a diffusing proton from the field of its conjugate base, we have found that simple exponential decay does not fit the observed kinetics. Rather, we have developed a two-step scheme in the experimental and theoretical studies of reversible ESPT processes in solutions (Scheme 1).[5] Here we give only briefly the details of this approach. The first step involves protolytic dissociation to form a solvent−ion pair with intrinsic rate constant k_d. The solvent−ion pair can undergo both adiabatic and nonadiabatic (proton quenching) recombination with rate constants k_a and k_q, respectively. The reversible reaction within the contact ion pair is followed by a diffusion second step in which the hydrated proton is removed from the parent molecule. The diffusion separation of proton and the excited anion is described by DSE with the characteristic constants $D = D_{H^+} + D_{R^*O^-}$, the mutual diffusion coefficients of the proton and the conjugated base, and $R_D \equiv |z_1 z_2| e^2/k_B T\epsilon$, the Debye radius. The latter defines the Coulombic attraction potential $V(r) = -R_D/r$. The overall reaction involves electronically excited species, and thus, one should consider the fluorescence lifetimes: $1/k_0 = \tau_0$ for the acid, $1/k_0' = \tau_0'$ for the base, and $1/k_0'' = \tau_0''$ for the contact ion pair. Usually, τ_0'' is much longer than that for all other chemical and diffusion processes and can be ignored. A more detailed description of Scheme 1 and method for kinetic parameters determination is given in the series of our preceding publications.[28,29]

In contrast to the kinetic behavior of naphthols, we need to introduce one more adjustable parameter to fit adequately the time-resolved signal of the conjugated base R^*O^-. It was predicted theoretically[29b] and demonstrated experimentally[29c] that the effective nonadiabatic recombination (proton quenching) leads to a nonexponential decay of R^*O^- fluorescence signal. However, we were unable to simultaneously fit the fluorescence kinetics of protonated and deprotonated form of **10-CPT** using tabulated values of the Debye radii and diffusion coefficients that we derived earlier[28] for single-charged anion of **10-CPT** (see curve b in Figure 9). A very good fit was achieved when we used a larger value of the Debye radii (see Table 1 and curve a in Figure 9), meaning a stronger Coulombic attraction than predicted for a singly charged proton and the monoanion of **10-CPT**. This suggests that the effective charge of the excited anion is more than |−1|, which is in good agreement with our

(28) Solntsev, K. M.; Huppert, D.; Agmon, N.; Tolbert, L. M. *J. Phys. Chem. A* **2000**, *104*, 4658−4669.

(29) (a) Gopich, I. V.; Solntsev, K. M.; Agmon, N. *J. Chem. Phys.* **1999**, *110*, 2164−2174. (b) Agmon, N. *J. Chem. Phys.* **1999**, *110*, 2175−2180. (c) Solntsev, K. M.; Agmon, N. *Chem. Phys. Lett.* **2000**, *320*, 262−268.

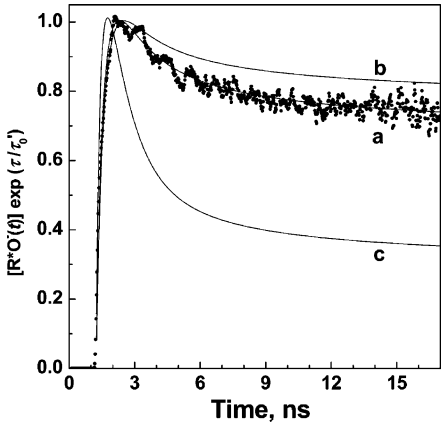

Figure 9. Time-resolved kinetics of R*O$^-$ from Figure 5. (a) Data and numerical solution of the DSE using the effective Debye radius. (b) Solution of the DSE using the theoretical Debye radius for this mixture. (c) Solution of the DSE using the Debye radius 2 times larger than theoretical. See text for details.

data on lactone ring hydrolysis in **10-CPT** and other **CPT** derivatives,[15−18] since the carboxylate form of **10-CPT** is doubly charged after deprotonation.

4.3. Ultrafast Processes. While the DSE treatment provides an adequate description for proton diffusion from a photoexcited acid, more recently we have discovered significant mechanistic information in the ultrafast time range.[21] In the current work, the direct proton-transfer rate between the **10-CPT** and water was measured using a pump−probe technique with ∼150 fs time resolution. We attributed the positive part of the signal to absorption due to the optical transition ROH(S_1) → ROH(S_2). The negative component arose from the R*O$^-$-stimulated emission due to transition to the ground state. The total signal at 590 nm was analyzed by

$$-\Delta T \propto \sigma_{\mathrm{ROH}^*} S(t) - \sigma_{\mathrm{R}^*\mathrm{O}^-}(1 - S(t)) + A \exp(-t/\tau_{\mathrm{short}}) \quad (1)$$

where σ_{ROH^*} denotes the absorption cross section of the S_1 to a higher excited-state $S_1 \rightarrow S_n$ transition of ROH and $\sigma_{\mathrm{R}^*\mathrm{O}^-}$ denotes the emission cross section of R*O$^-$. $S(t)$ and $(1 - S(t))$ are the excited-state survival probabilities of R*OH and R*O$^-$, respectively, which are calculated by the SSDP program. At our time frame, the $\sigma_{\mathrm{ROH}^*}S(t)$ component can be considered as ultrafast, and therefore, all time-dependent signals appear from $\sigma_{\mathrm{R}^*\mathrm{O}^-}(1 - S(t)) + A \exp(-t/\tau_{\mathrm{short}})$. To make correlations with TCSPC measurements, we can mention that the data in Figure 6 correspond to the first 50 ps of R*O$^-$ buildup in Figure 5. The short component, τ_{short}, arises from changes in both σ_{ROH^*} and $\sigma_{\mathrm{R}^*\mathrm{O}^-}$, and its origin is probably related to ultrafast hydrogen-bonded complex formation. The fits to the signals with the above-mentioned time components are shown in Figure 6 as solid lines, and the proton-transfer rate and the relevant parameters are given in Table 1.

The time-resolved fluorescence signal of 8-hydroxy-1,3,6-pyrenetrisulfonate (**HPTS**) in water using the up-conversion technique measured by Tran-Thi and co-workers[30] also exhibited short time components prior to the actual proton-transfer process, which takes a much longer time $k_d \approx (100\ \mathrm{ps})^{-1}$. The fast components were attributed to solvation dynamics and to a specific solute−solvent hydrogen bond formation. The long component of 87 ps fits approximately to the fluorescence decay of R*OH and to the growth of the fluorescence of R*O$^-$ measured by time-correlated single-photon counting techniques. Solvation dynamics measurements of Coumarin 343 dye in water[31] and Rhodamine 800 dye in water[32] have shown that solvation is a bimodal process with long components approximately equal to water and D_2O dielectric relaxation times.[33] It is plausible that hydrogen-bond formation or breaking has a range of time scales depending on the nature of both solute and solvent and whether a weak hydrogen bond already exists as mentioned above. In photoacids such as 2-naphthol and its derivatives, the ground-state ROH species already exhibit a hydrogen bond.[34] Upon excitation of **10-CPT**, the change in the charge distribution and bond lengths will probably affect this preexisting hydrogen bond at much shorter times. The fact that the short component of 3 ps exists in the signal of both R*OH and R*O$^-$ of **10-CPT** (data for R*OH is not shown) is in favor of the assignment to nonspecific solvation. More experiments are needed to clarify this important point. At present we cannot conclusively assign the origin of the fast component in the pump−probe signal shown in Figure 6.

4.4. The pH and Water Concentration Dependence. In the acidic region the prototropic behavior of **10-CPT** also differs from that of **6HQ** and is even more intriguing. As was mentioned earlier, the increased emission from **6HQ** cation is caused not by the shift of excited-state C*−T* equilibrium, but by the decreased activity of water acting as proton acceptor. Let us analyze the possible reasons for the observed prototropic behavior of **10-CPT**.

It was established from the kinetic data that the pK_a* of **10-CPT** in 1/1 v/v MeOH−H_2O mixture is around 0 (Table 1). Therefore, the observed transition with apparent pK_a* around 2 is not the result of R*OH ↔ R*O$^-$ + H$^+$ equilibrium. On the other hand, this equilibrium is about 1 pK_a unit higher than the ground-state N-protonation (Figure 3), and therefore, static quenching could also be ruled out.

As was mentioned earlier, a minor increase in basicity was detected for the **CPT** after excitation. Interestingly, the difference between ground- and excited-state pK_a* for deprotonation of the excited **CPT** quinolinium is approximately the same as the difference between ground-state pK_a for the "$>NH^+ \leftrightarrow >N$" transition and the unknown transition at pH 2 for **10-CPT**. Taking into account the fact that emission spectra did not change with the subsequent addition of an acid to the solution, we may speculate that the weak emission at 520 nm comes from the zwitterion (or tautomer) of **10-CPT**.

The dependence of ESPT rate constants on the solvent composition and pK_a* in methanol−water mixtures has been analyzed by us previously.[28] Therefore, in the current work we base our assumptions on the background developed earlier. The dissociation rate coefficient, k_d, depends nonlinearly on the mole fraction of water (Graph 1 in Figure 10), showing a strong

(30) Tran-Thi, T.-H.; Gustavsson, T.; Prayer, C.; Pommeret, S.; Hynes, J. T. *Chem. Phys. Lett.* **2000**, *329*, 421−430.
(31) Jimenez, R.; Fleming, G. R.; Kumar, P. V.; Maroncelli, M. *Nature* **1994**, *309*, 471−473.
(32) Zolotov, B.; Gan, A.; Fainberg, B. D.; Huppert, D. *J. Lumin.* **1997**, *72*−*74*, 842−844.
(33) Bertolini, D.; Cassettari, M.; Salvetti, G. *J. Chem. Phys.* **1982**, *76*, 3285−3290.
(34) (a) Solntsev, K. M.; Huppert, D.; Tolbert, L. M.; Agmon, N. *J. Am. Chem. Soc.* **1998**, *120*, 7981−7982. (b) Solntsev, K. M.; Huppert, D.; Agmon, N. *J. Phys. Chem.* **1999**, *103*, 6984−6997.

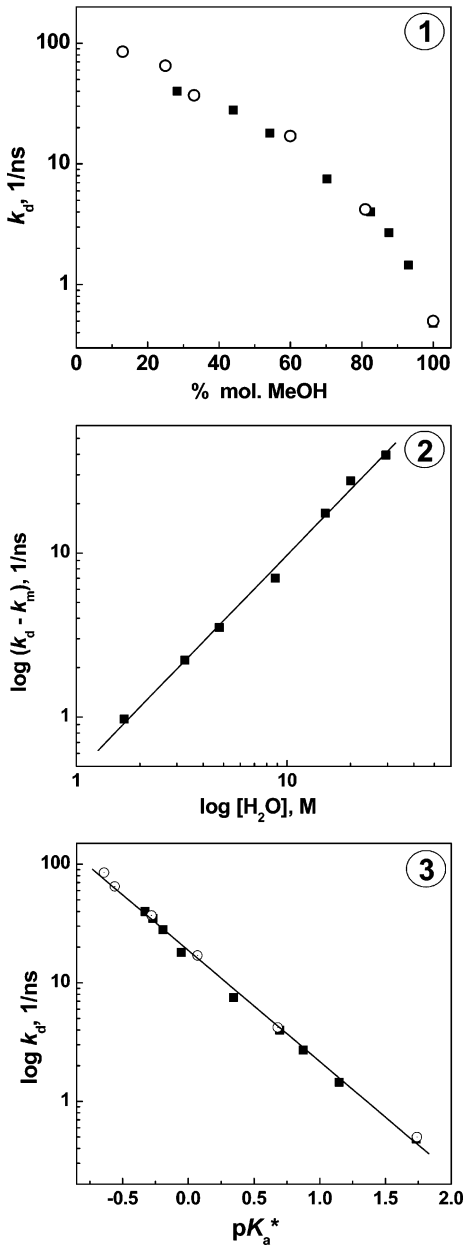

Figure 10. Dependence of dissociation rate constant k_d on solvent properties, (■) Data measured using TCSPC technique. Straight lines represent linear regression fits. (○) Data measured by pump−probe technique. (1) k_d vs solvent composition. (2) k_d vs molar water concentration in methanol−water mixtures. (3) Brønsted-type dependence of log k_d on the pK_a*, determined at different MeOH/H_2O ratios.

variation in the methanol-rich region and changing moderately in the water-rich region. A similar effect was observed for 5-cyano-2-naphthol[28] and 5-cyano-1-naphthol.[35] It was explained by (a) preferential solvation of the hydroxyl moiety by water and (b) gradual change in the solvation energy of the CIP.

Previously we suggested analyzing the water dependence of k_d using the assumption that ESPT to water and methanol can be considered as two parallel processes. In this case the nature of the proton-accepting water cluster can be determined by an analysis of the dissociation constant dependence on water concentration using

$$k_d = k_m + k_w[H_2O]^n \quad (2)$$

where k_m is the dissociation rate in pure methanol and k_w is its water dependent component, and n can be roughly associated with the number of water molecules involved in the proton-transfer step. We have found a correlation between the photoacid strength and the size of water cluster acting as primary proton acceptor.[28] The apparent size of the water cluster n decreased from 2.0 for **HPTS** with pK_a* = 1.4 down to 0.8 for 5,8-dicyano-2-naphthol with pK_a* ≈ −4.5. Our results show that for **10-CPT** n is about 1.3 (graph 2 in Figure 10) and pK_a* ≈ −0.7. Therefore, we confirm the above-mentioned hypothesis that n probably reflects the structure of the contact ion pair that may vary for the photoacids with different pK_a*'s.

Graph 3 in Figure 10 demonstrates the Brønsted-type dependence. The dissociation rate dependence on the free energy of the reaction shows a good linear correlation with a slope of 0.94 ± 0.02. This demonstrates that the ESPT from **10-CPT** to methanol−water mixtures is in endothermic regime for all water concentrations and our fastest determined k_d for this system (85 ps^{-1}) is still far from the rate-limiting factor for protolytic photodissociation in water. The characteristic time of the latter is usually assumed to be several picoseconds, between the Debye and longitudal relaxation times in water.[28]

5. Conclusions

As we have demonstrated previously, the acidity of hydroxyarenes shows a unique dependence on the structure of the photoacid. The antitumor agent 10-hydroxycamptothecin joins the class of photoacids with remarkable excited-state acidity, combining the kinetic efficiency of a hydroxyquinoline without its energy-wasting tautomerization and allowing access to more instrumentally accessible wavelengths. Although this study did not specifically examine **TPT**, we assume that its prototropic behavior mirrors many of these same properties, with the additional presence of an internal base. The result is that the efficient intramolecular proton transfer results in emission only from the conjugate base.[18d] Such intramolecular excited-state proton-transfer studies have been the subject of earlier studies.[36]

Acknowledgment. Support of this research by the U.S. National Science Foundation (Grant CHE-0096941) and the U.S.−Israel Binational Science Foundation is gratefully acknowledged.

JA047821E

(35) Pines, E.; Pines, D.; Barak, T.; Magnes, B.-Z.; Tolbert, L. M.; Haubrich, J. E. *Ber. Bunsen. Phys. Chem.* **1998**, *102*, 511−517.

(36) (a) Köhler, G.; Wolschann, P. *J. Chem. Soc., Faraday Trans. 2* **1987**, *83*, 513−527. (b) Tolbert, L. M.; Nesselroth, S. M. *J. Phys. Chem.* **1991**, *95*, 10331−10336. (c) de Bekker, E. J. A.; Pugzlys, A.; Varma, C. A. G. O. *J. Phys. Chem. A* **2001**, *105*, 399−409.